Letter

Coexistence of superconductivity and superionicity in Li_2MgH_{16}

Haoran Chen[1] and Junren Shi[1,2,*]

[1]*International Center for Quantum Materials, Peking University, Beijing 100871, China*

[2]*Collaborative Innovation Center of Quantum Matter, Beijing 100871, China*

(Received 15 May 2023; revised 21 August 2023; accepted 29 March 2024; published 15 April 2024)

We study superconductivity in the superionic phase of the clathrate hydride Li_2MgH_{16}, where hydrogen ions diffuse among the lattice formed by lithium and magnesium ions. By employing the stochastic path-integral approach, we nonperturbatively take into account the effects of quantum diffusion and anharmonic vibrations. Our calculations reveal strong electron-ion coupling [$\lambda(0) = 3.7$] and a high superconducting transition temperature (T_c) of 277 K under 260 GPa, at which the material is still superionic. T_c is significantly suppressed compared with the result $T_c = 473$ K obtained from the conventional approach based on the harmonic approximation. Our study, based on a first-principles approach applicable to superionic systems, indicates that the superconductivity and superionicity can coexist in Li_2MgH_{16}.

DOI: 10.1103/PhysRevB.109.L140505

Introduction. Superconductivity is one of the most fascinating phenomena in condensed matter physics. The Bardeen-Cooper-Schrieffer (BCS) theory first explains the underlying microscopic mechanism, revealing the important role of ion motion in inducing superconductivity. The theory predicts that a system tends to exhibit high superconducting transition temperature T_c if it has high phonon frequencies and strong electron-phonon coupling (EPC). In the past decade, the idea has inspired the theoretical predictions and experimental discoveries of hydride high-T_c superconductors under high pressures, with transition temperatures approaching or even exceeding room temperature [1–8]. The theoretical investigations usually rely on the harmonic approximations. However, in these systems, the motions of hydrogen ions can significantly deviate from harmonic vibrations, violating the underlying assumption of conventional approaches. For example, the crystal structure and T_c of hydride sulfide H_3S, an experimentally observed high temperature superconductor, cannot be determined correctly if anharmonic and quantum effects of hydrogen ions are neglected [9–11]. Moreover, quantum effects may cause metallic hydrogen to melt at a temperature below T_c, resulting in a superconducting liquid [12–17].

When anharmonic or quantum effects are strong, an intriguing dynamically disordered phase named superionic phase, which is characterized by the diffusion of some ions among the lattice formed by others, may emerge. The property is widely exploited in solid-state electrolytes [18–20]. It is also related with several dynamical phases of ice and is vital to understanding the phase diagram of water [21–26]. It is natural to ask whether the novel state can coexist with superconductivity. In recent years, some lithium alloys and clathrate superhydrides are found to possess both properties. However, superionicity in these materials occurs at temperatures much higher than the superconducting transition temperatures [4,27–30]. It is not yet known whether there is a material where superconductivity and superionicity could coexist in a certain temperature regime [31,32]. Li_2MgH_{16} is a promising candidate for realizing the coexistence. According to harmonic calculations, the $Fd\bar{3}m$ phase of the material is predicted to possess strong EPC and a T_c as high as 473 K at 250 GPa [33]. However, later studies based on path-integral molecular dynamics (PIMD) simulations reveal that anharmonicity and quantum effects drive the material to be superionic above 25 K, with hydrogen ions diffusing between sites [32]. This makes the prediction of harmonic calculations unreliable. A first-principles determination of T_c is hindered by the limitation of conventional computational approaches based on harmonic approximations.

In this Letter, we present a first-principles investigation of superconductivity in the superionic phase of Li_2MgH_{16}. To take into account the effects of anharmonic vibrations, quantum fluctuations, and ion diffusion, we apply the stochastic path-integral approach (SPIA), which is a nonperturbative approach without making assumptions of the nature of ion motion [11–13,34]. We study the electronic structure, electron-ion coupling, and superconductivity in the superionic Li_2MgH_{16}. We find that the electronic structure is strongly renormalized by ion diffusion and the coupling between electrons and ions is strong. Notably, we observe that the material has a high $T_c = 277$ K, at which it is superionic. Therefore, superconductivity and superionicity can coexist in the system.

Ion motion. We begin by examining the ion motion in Li_2MgH_{16}. To fully take into account the effect of anharmonicity and quantum tunneling, we perform PIMD simulations [35,36]. The interaction between ions is described with a machine-learning force field (MLFF). Following the original spirit of Refs. [37,38], the potential field is first trained on the fly in MD simulations, followed by an

*junrenshi@pku.edu.cn

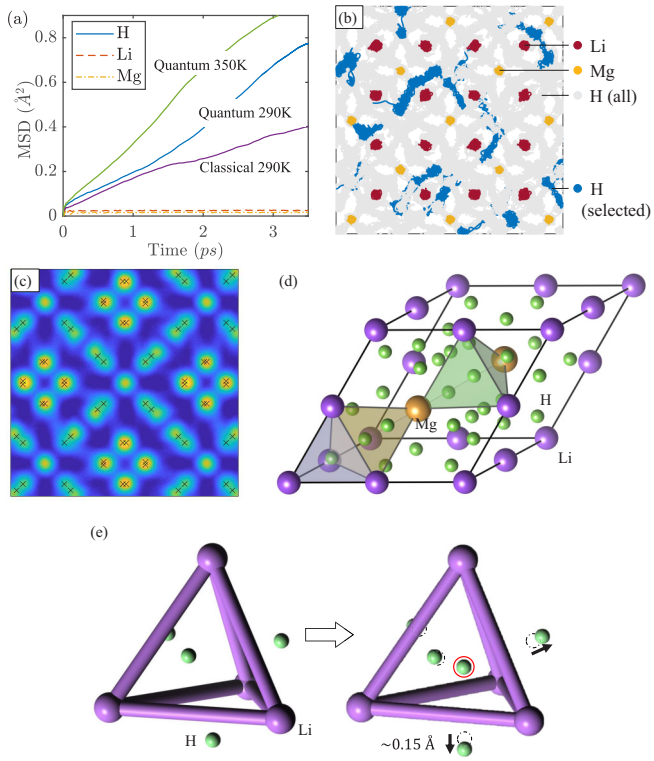

FIG. 1. (a) Mean squared displacement (MSD) of hydrogen (blue solid line), lithium (red dashed line), and magnesium (yellow dot-dashed line) ions under 260 GPa at 290 K. MSD of hydrogen ions from classical MD simulation at 290 K and PIMD simulation at 350 K are also shown for comparison. (b) [100] view of trajectories of centroid mode of all hydrogen (gray), lithium (red), and magnesium (yellow) ions. Selected trajectories of hydrogen ions are marked by blue lines. (c) [100] view of density distribution of hydrogen ions from a PIMD simulation. Hydrogen ions of the solid phase are marked with cross marks. (d) The effective "crystal structure" of the superionic phase. The structure is made up of three basic components: Li_4 (gray), Li_3Mg (yellow), and Li_2Mg_2 (green) tetrahedra, with hydrogen ions occupying their centers. (e) A schematic illustration of the effective structural transition around the Li_4 tetrahedra from solid phase (left) to superionic phase (right). In the right panel, the previously empty 8b site is circled in red solid line.

on-the-fly PIMD training. Detailed descriptions can be found in the Supplemental Material [39].

In the PIMD simulation, each quantum ion is mapped to a classical ring polymer [40]. In Fig. 1(b), we show the trajectories of the center of mass of the ring polymers at 290 K, from which the mean squared displacements (MSD) of ions are determined. It can be seen that all lithium and magnesium ions keep vibrating around their equilibrium positions, while hydrogen ions diffuse among the Li_2Mg lattice. Correspondingly, the MSD of hydrogen ions keeps increasing, while those of lithium and magnesium ions remain around zero. On average, the diffusion coefficient of hydrogen ions is 3.7×10^{-6} cm^2/s at 290 K. Compared with the classical molecular dynamics result 1.9×10^{-6} cm^2/s, quantum effects accelerates the ion diffusion by about two times [41].

To further probe how the dynamical ions arrange in the system, we analyze the hydrogen density distributions. From

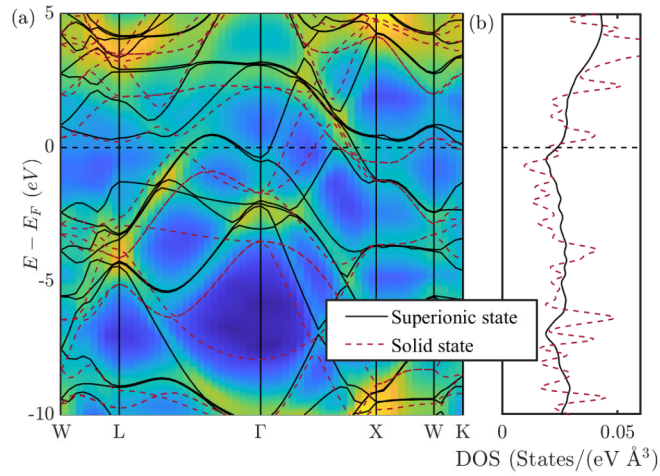

FIG. 2. (a) Partial density of states $\rho(\boldsymbol{k}, E)$ in the IBZ calculated under quasistatic approximation (mapped into colors in the background) and band structure solved from the effective Hamiltonian (black solid lines) in the superionic phase. Band structures in the solid phase (red dashed lines) are shown for comparison. (b) DOS in the two states. The superionic one is calculated using eigenvalues from all configurations.

Fig. 1(c), we see that density peaks form periodical structures and are connected with each other by almost straight paths. It appears that, instead of freely diffusing in the latticelike liquids, hydrogen ions tend to hop between sites. By fitting the density distribution to three-dimensional Gaussian functions, we extract the effective "crystal structure" of the superionic phase, as shown in Fig. 1(d). We find that the structure is almost identical to the solid phase, with hydrogen occupying 32e and 96g sites at the center of Li_3Mg and Li_2Mg_2 tetrahedra. Now, the previously empty 8b sites at the center of Li_4 tetrahedra are also occupied. This is consistent with Wang *et al.*'s observations in Ref. [32]. Due to the occupation, the hydrogen tetrahedron around it formed by ions at 32e sites is pushed slightly larger [see Fig. 1(e)]. The site coordinates are listed in Table S1 [39]. The new crystal structure still obeys the symmetry of the $Fd\bar{3}m$ space group.

Renormalized electronic structure. We then study the electronic structure of the system. As analyzed above, while some ions diffuse between sites, the sites form a solidlike periodic framework. As a result, the system still has discrete translational symmetry and electron states can be labeled by a wave vector $\boldsymbol{k}$ in the irreducible Brillouin zone (IBZ) of the primitive cell [42,43]. The band structure can be extracted from the partial density of states (DOS) $\rho(\boldsymbol{k}, E)$ at $\boldsymbol{k}$:

$$\rho(\boldsymbol{k}, E) = \frac{1}{2\pi} \mathrm{Tr}_{\sigma} A(\boldsymbol{k} + \boldsymbol{G}, \boldsymbol{k} + \boldsymbol{G}', E), \tag{1}$$

where $\hat{A}(E)$ is the electron spectral function and $\boldsymbol{G}(\boldsymbol{G}')$ is a reciprocal lattice vector of the primitive cell. To see the qualitative properties of the band structure of Li_2MgH_{16}, we calculate $\rho(\boldsymbol{k}, E)$ under the quasistatic approximation, i.e., instantaneous spectral functions are averaged over all ion configurations [39,43]. The result is shown in Fig. 2(a). As expected, the band structure is strongly renormalized by ion diffusion and becomes qualitatively different from that in solid

phase. The full DOS is shown in Fig. 2(b). We see that DOS at the Fermi surface is slightly lifted from 0.020 states/(eV Å^3) to 0.024 states/(eV Å^3) compared with the solid phase. Both values are high and are likely to support a large λ and a high T_c.

On the other hand, due to the coupling with fluctuating ions, each band acquires a finite width, which is related to the inverse lifetime of quasielectrons. From the approximated $\rho(\boldsymbol{k}, E)$, we find that the half width γ is about 0.51 eV for states near the Fermi surface, while the Fermi energy ε_F is about 23 eV. Compared with the anharmonic solid H_3S, where $\gamma \sim 0.16$ eV and $\varepsilon_F \sim 25$ eV, the half width are larger, but still much smaller than the Fermi energy. The observation indicates that long-lived quasielectrons persist in the system, although the ion fluctuation in Li_2MgH_{16} is much stronger than ordinary solids. This allows us to take a similar process of studying superconductivity as conventional theories. First, we study the propagation of quasielectrons in the normal state. Then we determine the effective attractive interaction induced by the coupling with moving ions (phonon in the case of ordinary solids).

The nonperturbative SPIA provides a good framework to perform such analysis [11–13,34]. In SPIA, we calculate the Green's function $\bar{\mathcal{G}}(i\omega_j)$ to describe the propagation of quasielectrons in normal states, where $\omega_j = (2j+1)\pi k_B T$ is a fermion Matsubara frequency (see the Supplemental Material [39] for details). Wave functions of the quasielectrons are then naturally defined to approximately diagonalize $\bar{\mathcal{G}}(i\omega_j)$, so that the waves can propagate in the system without being scattered. Generally, the Green's function has the structure $\bar{\mathcal{G}}(i\omega_j) = [i\omega_j - \hat{H}_{\rm kin} - \hat{\Sigma}(i\omega_j)]^{-1}$, where $\hat{H}_{\rm kin}$ is the kinetic energy and $\hat{\Sigma}$ is the electron self-energy. The Green's function is generally non-Hermitian and the eigenstates are thus not orthonormalized. Fortunately, the small inverse lifetime γ indicates a small anti-Hermitian part of $\hat{H}_{\rm kin} + \hat{\Sigma}$. Therefore, we can diagonalize an effective Hamiltonian $\hat{H}_{\rm eff} = \hat{H}_{\rm kin} + {\rm Re}\hat{\Sigma}(i\omega_j)$ to determine the wave functions of quasielectrons [11]. As the system is periodic, eigenstates of $\hat{H}_{\rm eff}$ take the form of Bloch waves. The obtained band structure is shown in Fig. 2(a). The dispersions coincide well with where the previously obtained $\rho(\boldsymbol{k}, E)$ peaks.

EPC parameters and superconductivity. We then study the superconductivity in the system. We focus on the pairing between time reversal states $1 \equiv (n, \boldsymbol{k}, i\omega_j)$ and $\bar{1} \equiv (n, -\boldsymbol{k}, -i\omega_j)$, where n and $\boldsymbol{k}$ are band and wave vector indices of the Bloch waves solved from $\hat{H}_{\rm eff}$. The pairing is induced by the effective attractive interaction $\hat{W}$ mediated by moving ions. In the framework of SPIA, $\hat{W}$ is determined by solving a Bethe-Salpeter equation,

$$W_{11'} = \Gamma_{11'} + \frac{1}{\hbar^2\beta}\sum_2 W_{12}|\bar{\mathcal{G}}_2|^2\Gamma_{21'}, \tag{2}$$

where $\Gamma_{11'} = -\beta\langle\mathcal{T}_{11'}\mathcal{T}_{\bar{1}\bar{1}'}\rangle$ is the fluctuation of T matrices of electron-ion scattering in PIMD simulations [44]. It describes the scattering amplitude of a time-reversal quasielectron pair from $(1, \bar{1})$ to $(1', \bar{1}')$ [11–13]. The EPC parameters $\lambda(j-j')$ are then defined as the summation of $\hat{W}$ over the Fermi surface, i.e.,

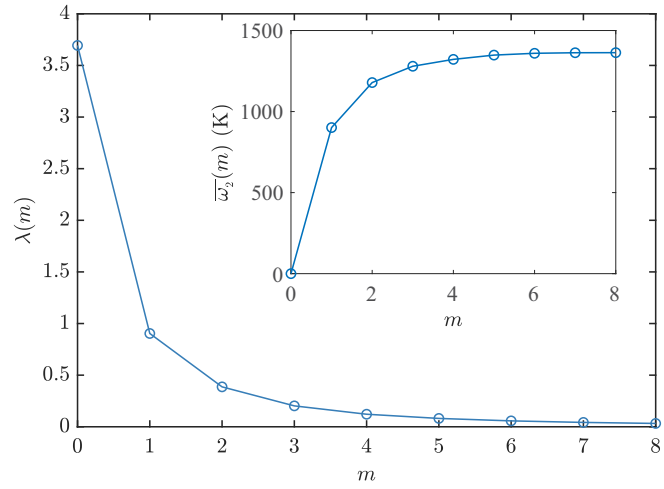

FIG. 3. EPC parameters $\lambda(m)$ of Li_2MgH_{16} under 260 GPa at 290 K, calculated on a $8\times8\times8$ k grid and $8\times8\times8$ q grid. Inset: the asymptotic behavior of $\bar{\omega}_2(m) = 2\pi/\hbar\beta\sqrt{m^2\lambda(m)/\lambda(0)}$. The value at infinity $\bar{\omega}_2(\infty)$ gives the EPC-weighted average phonon frequency [12,45]. The results are calculated using nondiagonal supercells, each containing 304 atoms [39].

$$\lambda(j-j') = -\frac{1}{N(\varepsilon_F)}\sum_{n\boldsymbol{k},n'\boldsymbol{k}'} W_{n\boldsymbol{k},n'\boldsymbol{k}'}(j-j') \times \delta(\varepsilon_{n\boldsymbol{k}} - \varepsilon_F)\delta(\varepsilon_{n'\boldsymbol{k}'} - \varepsilon_F), \tag{3}$$

where $j - j'$ represents a bosonic Matsubara frequency $\nu_{j-j'} = \omega_j - \omega_{j'}$ and $N(\varepsilon_F)$ is the DOS on the Fermi surface. Similar to conventional theories, the EPC parameters enter the linearized Eliashberg equations to determine T_c [39,45].

In practice, the Fermi surface summations in Eq. (3) require dense sampling of wave vector transfer $\boldsymbol{q} = \boldsymbol{k} - \boldsymbol{k}'$. The sampling is enabled by combining SPIA with MLFF [37], which makes simulations in large supercells computationally affordable, and the nondiagonal supercell technique [46], which uses smaller supercells to cover a dense q grid (see the Supplemental Material [39] for details). By applying the approaches, we find that the static EPC parameter $\lambda(0) = 3.7$. The value is close to that calculated in the solid phase $\lambda_{\rm solid}(0) \approx 4.0$ [33] and much higher than the previous estimated value $\lambda(0) = 1.6$ in the superionic phase [32]. Values of higher-frequency components are shown in Fig. 3. Using a typical Morel-Anderson Coulomb pseudopotential $\mu^* = 0.10$, we solve the linearized Eliashberg equations and find $T_c = 277$ K [47]. The value is much lower than the harmonic result $T_c = 473$ K in the low-temperature solid phase [33], but still close to the room-temperature regime. At the temperature, Li_2MgH_{16} is superionic, suggesting that the material is a superionic superconductor.

In the superionic metal, the behavior of ion motion is expected to be temperature dependent. For example, as shown in Fig. 1, the diffusion coefficient depends strongly on the temperature. To examine the sensitivity of the predicted T_c to the simulation temperature, we perform simulations at 350 K, which is 73 K higher than T_c. The diffusion coefficient is

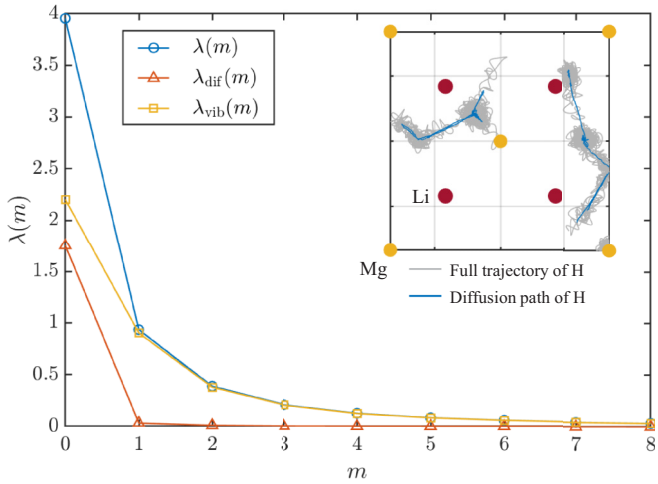

FIG. 4. Contributions of different types of ion motion to the EPC parameters $\lambda(m)$ under 260 GPa at 290 K. Inset: full trajectories and diffusion paths of two selected hydrogen ions obtained using a moving-average filter with 250 fs window length. The diffusion contribution $\lambda_{\rm dif}(m)$ is calculated from all such diffusion paths. The results are calculated in a supercell containing 76 atoms.

about 20% higher than that at 290 K. By assuming that the properties of ion motion do not change much at different temperatures, we represent EPC parameters $\lambda(m, T)$ as a single frequency-dependent function $\lambda(\nu_m(T))$ and interpolate it to obtain values at other temperatures (see Fig. S1 [39]). We find that the static EPC parameter $\lambda_{350\ \rm K}(0)$ is slightly suppressed to be 3.5, while T_c is overestimated by about 9 K (3% of T_c).

To better understand the results, it is natural to ask how different types of ion motion contribute to superconductivity in Li_2MgH_{16}. To answer the question, we perform further analysis in a smaller supercell containing 76 atoms. We assume that the ion trajectory can be expressed as the summation of diffusion paths and local vibrations around the path:

$$\boldsymbol{R}(t,\tau) = \boldsymbol{R}_{\rm dif}(t,\tau) + \Delta\boldsymbol{R}_{\rm vib}(t,\tau). \tag{4}$$

Since local vibrations are much faster than the diffusion, the diffusion path can be obtained by performing a moving average of ion trajectories (see inset of Fig. 4). We then calculate the contribution of pure diffusion to EPC parameters $\lambda(m)$. As shown in Fig. 4, diffusion contributes a large $\lambda_{\rm dif}(0) = 1.75$, but almost vanishing higher-frequency components. Subtracting $\lambda_{\rm dif}(m)$ from $\lambda(m)$, we obtain contributions from local vibrations and vibration-diffusion couplings. The predicted T_c is only slightly suppressed from 283 K to 275 K. Based on the observations, we conclude that the main effect of ion diffusion is to renormalize electron wave functions and band structures. The pairing between the electrons, however, is mainly induced by local vibrations. Diffusion greatly enhances $\lambda(0)$ but barely affects T_c. It indicates that a large $\lambda(0)$ is not a reliable predictor for T_c for superionic solids.

Summary. In summary, we systematically study the ion motion, electronic structure, and superconductivity in the superionic metal Li_2MgH_{16} using first-principles calculations. We find that, while the ions fluctuate much more strongly than conventional solids, long-lived quasielectrons persist in the system. The wave functions and band structures of quasielectrons are strongly renormalized. The pairing between the quasielectrons is analyzed using the nonperturbative SPIA method, so that all anharmonic effects like anharmonic local vibrations, quantum fluctuations, and ion diffusion are taken into account properly. By combining the SPIA method with MLFF and nondiagonal supercell techniques, we are able to calculate electron-electron effective interactions on sufficiently dense k grids and q grids in such a complex system. The superionic metal is predicted to have a large EPC parameter $\lambda(0) = 3.7$ and a high superconducting $T_c = 277$ K at 260 Gpa. Further analysis suggests that ion diffusion contributes to the large $\lambda(0)$, while pairing between electrons is mainly induced by local vibrations of ions. Our study predicts that Li_2MgH_{16} is a superionic superconductor.

We gratefully acknowledge H. Liu, J. Lv, and Y. Sun for valuable discussions. The authors are supported by the National Science Foundation of China under Grant No. 12174005 and the National Key R&D Program of China under Grants No. 2018YFA0305603 and No. 2021YFA1401900. The computational resources were provided by the High-performance Computing Platform of Peking University.

[1] H. Wang, J. S. Tse, K. Tanaka, T. Iitaka, and Y. Ma, Proc. Natl. Acad. Sci. USA **109**, 6463 (2012).
[2] D. Duan, Y. Liu, F. Tian, D. Li, X. Huang, Z. Zhao, H. Yu, B. Liu, W. Tian, and T. Cui, Sci. Rep. **4**, 6968 (2014).
[3] A. P. Drozdov, M. I. Eremets, I. A. Troyan, V. Ksenofontov, and S. I. Shylin, Nature (London) **525**, 73 (2015).
[4] H. Liu, I. I. Naumov, R. Hoffmann, N. W. Ashcroft, and R. J. Hemley, Proc. Natl. Acad. Sci. USA **114**, 6990 (2017).
[5] A. P. Drozdov, P. P. Kong, V. S. Minkov, S. P. Besedin, M. A. Kuzovnikov, S. Mozaffari, L. Balicas, F. F. Balakirev, D. E. Graf, V. B. Prakapenka, E. Greenberg, D. A. Knyazev, M. Tkacz, and M. I. Eremets, Nature (London) **569**, 528 (2019).
[6] P. Kong, V. S. Minkov, M. A. Kuzovnikov, A. P. Drozdov, S. P. Besedin, S. Mozaffari, L. Balicas, F. F. Balakirev, V. B. Prakapenka, S. Chariton, D. A. Knyazev, E. Greenberg, and M. I. Eremets, Nat. Commun. **12**, 5075 (2021).
[7] Z. Li, X. He, C. Zhang, X. Wang, S. Zhang, Y. Jia, S. Feng, K. Lu, J. Zhao, J. Zhang, B. Min, Y. Long, R. Yu, L. Wang, M. Ye, Z. Zhang, V. Prakapenka, S. Chariton, P. A. Ginsberg, J. Bass *et al.*, Nat. Commun. **13**, 2863 (2022).
[8] L. Ma, K. Wang, Y. Xie, X. Yang, Y. Wang, M. Zhou, H. Liu, X. Yu, Y. Zhao, H. Wang, G. Liu, and Y. Ma, Phys. Rev. Lett. **128**, 167001 (2022).
[9] I. Errea, M. Calandra, C. J. Pickard, J. Nelson, R. J. Needs, Y. Li, H. Liu, Y. Zhang, Y. Ma, and F. Mauri, Phys. Rev. Lett. **114**, 157004 (2015).
[10] I. Errea, M. Calandra, C. J. Pickard, J. R. Nelson, R. J. Needs, Y. Li, H. Liu, Y. Zhang, Y. Ma, and F. Mauri, Nature (London) **532**, 81 (2016).

[11] H. Chen and J. Shi, Phys. Rev. B **106**, 184501 (2022).
[12] H. Liu, Y. Yuan, D. Liu, X.-Z. Li, and J. Shi, Phys. Rev. Res. **2**, 013340 (2020).
[13] H. Chen, X.-W. Zhang, X.-Z. Li, and J. Shi, Phys. Rev. B **104**, 184516 (2021).
[14] J. M. McMahon and D. M. Ceperley, Phys. Rev. B **84**, 144515 (2011).
[15] J. Chen, X.-Z. Li, Q. Zhang, M. I. J. Probert, C. J. Pickard, R. J. Needs, A. Michaelides, and E. Wang, Nat. Commun. **4**, 2064 (2013).
[16] H. Y. Geng, R. Hoffmann, and Q. Wu, Phys. Rev. B **92**, 104103 (2015).
[17] J. E. Jaffe and N. W. Ashcroft, Phys. Rev. B **23**, 6176 (1981).
[18] S. Chandra, *Superionic Solids - Principles and Applications* (North-Holland, Amsterdam, 1981).
[19] N. Kamaya, K. Homma, Y. Yamakawa, M. Hirayama, R. Kanno, M. Yonemura, T. Kamiyama, Y. Kato, S. Hama, K. Kawamoto, and A. Mitsui, Nat. Mater. **10**, 682 (2011).
[20] Y. Wang, W. D. Richards, S. P. Ong, L. J. Miara, J. C. Kim, Y. Mo, and G. Ceder, Nat. Mater. **14**, 1026 (2015).
[21] M. Benoit, D. Marx, and M. Parrinello, Nature (London) **392**, 258 (1998).
[22] A. F. Goncharov, V. V. Struzhkin, H. K. Mao, and R. J. Hemley, Phys. Rev. Lett. **83**, 1998 (1999).
[23] A. F. Goncharov, N. Goldman, L. E. Fried, J. C. Crowhurst, I.-F. W. Kuo, C. J. Mundy, and J. M. Zaug, Phys. Rev. Lett. **94**, 125508 (2005).
[24] E. Schwegler, M. Sharma, F. Gygi, and G. Galli, Proc. Natl. Acad. Sci. USA **105**, 14779 (2008).
[25] M. Millot, F. Coppari, J. R. Rygg, A. Correa Barrios, S. Hamel, D. C. Swift, and J. H. Eggert, Nature (London) **569**, 251 (2019).
[26] Q.-J. Ye, L. Zhuang, and X.-Z. Li, Phys. Rev. Lett. **126**, 185501 (2021).
[27] H. Liu, I. I. Naumov, Z. M. Geballe, M. Somayazulu, J. S. Tse, and R. J. Hemley, Phys. Rev. B **98**, 100102(R) (2018).
[28] Z. Wan, W. Xu, T. Yang, and R. Zhang, Phys. Rev. B **106**, L060506 (2022).
[29] X. Wang, Y. Wang, J. Wang, S. Pan, Q. Lu, H.-T. Wang, D. Xing, and J. Sun, Phys. Rev. Lett. **129**, 246403 (2022).
[30] Z. Wan, C. Zhang, T. Yang, W. Xu, and R. Zhang, New J. Phys. **24**, 113012 (2022).
[31] H. Wang, P. T. Salzbrenner, I. Errea, F. Peng, Z. Lu, H. Liu, L. Zhu, C. J. Pickard, and Y. Yao, Nat. Commun. **14**, 1674 (2023).
[32] H. Wang, Y. Yao, F. Peng, H. Liu, and R. J. Hemley, Phys. Rev. Lett. **126**, 117002 (2021).
[33] Y. Sun, J. Lv, Y. Xie, H. Liu, and Y. Ma, Phys. Rev. Lett. **123**, 097001 (2019).
[34] X.-W. Zhang, H. Chen, E.-G. Wang, J. Shi, and X.-Z. Li, Phys. Rev. B **105**, 155148 (2022).
[35] D. Marx and M. Parrinello, J. Chem. Phys. **104**, 4077 (1996).
[36] M. Ceriotti, M. Parrinello, T. E. Markland, and D. E. Manolopoulos, J. Chem. Phys. **133**, 124104 (2010).
[37] R. Jinnouchi, F. Karsai, and G. Kresse, Phys. Rev. B **100**, 014105 (2019).
[38] R. Jinnouchi, J. Lahnsteiner, F. Karsai, G. Kresse, and M. Bokdam, Phys. Rev. Lett. **122**, 225701 (2019).
[39] See Supplemental Material at http://link.aps.org/supplemental/10.1103/PhysRevB.109.L140505 for numerical details, convergence tests, and some formulas that are applied in our calculations, which includes Refs. [49–55].
[40] D. Chandler and P. G. Wolynes, J. Chem. Phys. **74**, 4078 (1981).
[41] Both quantum and classical diffusion coefficients are obtained from simulations using (path-integral) Langevin thermostats and are only used to schematically demonstrate the quantum effect of hydrogen ions. To correctly calculate the real-time dynamical properties, average over classical *NVE* simulations and quantum techniques like ring-polymer molecular dynamics or centroid molecular dynamics are necessary [32,48]. When calculating T_c using SPIA, only imaginary-time information is necessary and can be correctly captured using Langevin thermostats.
[42] P. B. Allen, T. Berlijn, D. A. Casavant, and J. M. Soler, Phys. Rev. B **87**, 085322 (2013).
[43] M. Zacharias, M. Scheffler, and C. Carbogno, Phys. Rev. B **102**, 045126 (2020).
[44] G. D. Mahan, *Many-Particle Physics* (Kluwer Academic, Dordrecht, 2000).
[45] P. B. Allen and R. C. Dynes, Phys. Rev. B **12**, 905 (1975).
[46] J. H. Lloyd-Williams and B. Monserrat, Phys. Rev. B **92**, 184301 (2015).
[47] In solving the Eliashberg equation, the Morel-Anderson pseudopotential is renormalized with respect to the cutoff $\omega_N = 2\pi N k_B T$ to be $1/\mu^*(N) = 1/\mu^* + \ln(\overline{\omega_2}/\omega_N)$ [45]. This guarantees that T_c does not rely on the energy cutoff. In our calculations, $\mu^* = 0.16 - 0.10$ leads to $T_c = 236$–277 K.
[48] X. Li and E.-G. Wang, *Computer Simulations of Molecules and Condensed Matter: From Electronic Structures to Molecular Dynamics*, Peking University–World Scientific Advance Physics Series No. 3 (World Scientific, Hackensack, NJ, 2018).
[49] A. B. Migdal, Zh. Eksp. Teor. Fiz. **34**, 1438 (1958).
[50] D. J. Scalapino, in *Superconductivity: (in two volumes)*, edited by R. D. Parks (Marcel Dekker, New York, 1969).
[51] P. E. Blöchl, Phys. Rev. B **50**, 17953 (1994).
[52] G. Kresse and D. Joubert, Phys. Rev. B **59**, 1758 (1999).
[53] G. Kresse and J. Furthmüller, Phys. Rev. B **54**, 11169 (1996).
[54] J. P. Perdew, K. Burke, and M. Ernzerhof, Phys. Rev. Lett. **77**, 3865 (1996).
[55] F. Giustino, Rev. Mod. Phys. **89**, 015003 (2017).